APPLIED ORGANOMETALLIC CHEMISTRY
Appl. Organometal. Chem. 2005; **19**: 778–789
Main Group Metal Compounds
Published online 22 March 2005 in Wiley InterScience (www.interscience.wiley.com). DOI:10.1002/aoc.892

Structural and physicochemical characterization of zinc(II) and cadmium(II) complexes with 1,4-dimethy-lhomopiperazine

Yuki Matsunaga, Kiyoshi Fujisawa*, Nagina Amir, Yoshitaro Miyashita and Ken-ichi Okamoto

Graduate School of Pure and Applied Sciences, University of Tsukuba, Tsukuba 305-8571, Japan

Received 15 November 2004; Revised 20 December 2004; Accepted 22 December 2004

In order to know the relationship between structures and physicochemical properties of Group 12 metal(II) ions, the complexes with 'simple' ligands, such as alkyl cyclic diamine ligand and halide ions, were synthesized by the reaction of 1,4-dimethylhomopiperazine (hp′) with MX_2 as metal sources (M = Zn, Cd; X = Cl, Br, I). The five structural types, $[ZnX_2(hp')]$ (X = Cl (1), Br (2) and I (3)), $[ZnX_3(Hhp')]$ (X = Cl (1′) and Br (2′)), $[CdCl_2(hp')]_n$ (4), $[\{CdCl_2(Hhp')\}_2(\mu\text{-}Cl)_2]$ (4′) and $[\{CdX(hp')\}_2(\mu\text{-}X)_2]$ (X = Br (5), I (6)), were determined by X-ray analysis. The sizes of both metal(II) and halide ions and the difference in each other's polarizability influence each structure. All complexes were characterized by IR, far-IR, Raman and UV–Vis absorption spectroscopies. In the far-IR and Raman spectra, the typical ν(M–N) and ν(M–X) peaks clearly depend on the five structural types around 540–410 cm^{-1} and 350–160 cm^{-1} respectively. The UV–Vis absorption band energy around 204–250 nm also reflects each structural type. Copyright © 2005 John Wiley & Sons, Ltd.

KEYWORDS: crystal structure; zinc; cadmium; far-IR frequency; Raman shift; CT transition

INTRODUCTION

Group 12 metal(II) ions, such as zinc(II) and cadmium(II) ions, have a stable d^{10} electronic configuration. For this reason, no absorption bands in the visible region are observed, i.e. these compounds have no color.[1–5] Therefore, it is difficult to identify their coordination atoms and structural geometry by using absorption spectra in the visible region. We have to use X-ray analysis just to know the coordination geometry around metal(II) ions in the case of Group 12 metal(II) complexes. In spite of the present situation, the systematic examination of vibration energies and charge-transfer (CT) transition energies has not been well studied. There are only a few reports for the physicochemical properties and coordination modes of Group 12 metal(II) ions.[6–15]

*Correspondence to: Kiyoshi Fujisawa, Graduate School of Pure and Applied Sciences, University of Tsukuba, Tsukuba 305-8571, Japan.
E-mail: kiyoshif@chem.tsukuba.ac.jp
Contract/grant sponsor: Japan Society for the Promotion of Science; Contract/grant numbers: 13555257; 14350471.
Contract/grant sponsor: Ministry of Education, Culture, Sports, Science and Technology.

In addition, zinc and cadmium metals are trace elements in biological systems,[1–5,16] and zinc(II) and cadmium(II) complexes have been studied from the viewpoint of antimicrobial activity.[17] Many model complexes have already been reported; however, most of them are useful only as structural models and not for spectroscopic characterization, since the ligands contain an aromatic ring to stabilize the complexes.[18–22] We expect that complexes containing only 'simple' supporting ligands would make up for this disadvantageous point. The word 'simple' means that they do not contain double or triple bonds and have a low molecular weight. We have studied the physicochemical properties of the Group 12 metal(II) complexes with 'simple' supporting ligands, using spectroscopic methods such as UV–Vis absorption, IR, far-IR and Raman spectroscopies. The complexes containing these 'simple' supporting ligands give two direct pieces of information about the central metal(II) ions. First, no $n \rightarrow \sigma^*$ or $\sigma \rightarrow \sigma^*$ transition bands in the ligands region are observed in the near UV; therefore, the absorption bands reflect their coordination modes and atoms in the near-UV region. Second, the vibration bands in IR and far-IR regions can be easily assigned. It is clear that the Group 12 metal(II) complexes with

sulfur-containing 'simple' ligands, such as 1-cyclohexanethiol and 1-adamantanethiol, are very easy to assign vibration energies and CT transition energies, depending on the central metal(II) ions and coordination modes.[23] The physicochemical properties obtained by using 'simple' supporting ligands are useful for research on metalloproteins and complexes containing zinc(II) and cadmium(II) ions. In particular, ν(M–L) energies in far-IR and Raman spectra and CT transition energies in UV–Vis spectra could be good indicators for their coordination environment.

Recently, some complexes using nitrogen-containing 'simple' ligands, such as 1-methylpiperazine and 1,4-dimethylpiperazine, with cobalt(II),[24–26] nickel(II),[25] copper (II),[25,27] zinc(II)[25,28] and platinum(II)[29,30] ions have been reported. Homopiperazine (referred to as hp) complexes with copper(II),[31,32] platinum(II)[33,34] and copper(II)/zinc(II) ions[35] have also been reported. These cyclic diamine ligands, such as piperazine (containing a six-membered ring), homopiperazine (containing a seven-membered ring) and their analogues, coordinate in monodentate or didentate fashion.

Before using 1,4-dimethylhomopiperazine (referred to as hp′), we synthesized the zinc(II) and cadmium(II) complexes with hp as a 'simple' supporting ligand. The reactions of metal(II) halides with homopiperazine give an insoluble powder immediately, $[MX_2(hp)]_n$ (M = Zn, Cd; X = Cl, Br, I). Therefore, we cannot discuss their structures. In the next step, we pay attention to hp′ to increase its solubility by introduction of a methyl substitution group on nitrogen atoms (Scheme 1). Moreover, no zinc(II) and cadmium(II) complexes with hp′ ligand have been reported yet, to our knowledge. In this regard, we report herein the zinc(II) and cadmium(II) complexes with hp′ in comparison with analogous piperazine complexes. All the structures are determined by X-ray analysis. Their physicochemical properties are characterized by IR, far-IR, Raman and UV–Vis spectroscopies.

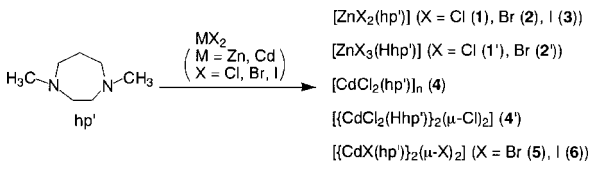

Scheme 1.

MATERIALS AND METHODS

General considerations

$ZnCl_2$, $ZnBr_2$, ZnI_2, $CdCl_2{\cdot}2.5H_2O$, $CdBr_2{\cdot}4H_2O$ and CdI_2 were obtained from Wako Pure Chemical Int. Ltd. Homopiperazine was obtained from Aldrich Chemical Company, Inc. $CDCl_3$ and D_2O were purchased from Cambridge Isotope Laboratories, Inc. All chemical reagents were used without further purification. Preparation and handling of all the complexes were performed under an argon atmosphere by employing standard Schlenk line techniques. MeOH, EtOH and 2-propanol were commercial spectroscopic grade and used after bubbling with argon gas.

IR and far-IR spectra were respectively recorded using KBr pellets in the 4600–400 cm^{-1} region and CsI pellets in the 650–150 cm^{-1} region on a JASCO FT/IR-550 spectrophotometer. FT-Raman spectra were measured using KBr or neat pellets in the 650–150 cm^{-1} region on a Perkin Elmer Spectrum GX spectrophotometer. UV–Vis spectra of the solution state were recorded on a JASCO V-570 spectrophotometer at room temperature using a quartz cell (1 mm path length) in the 200–500 nm region. UV–Vis spectra of the solid state were recorded on a JASCO V-560 spectrophotometer in the 200–500 nm region using the fine powder mull samples, which were prepared by finely grinding the solid materials. These were suspended in mineral oil (poly(dimethylsiloxane), Aldrich) and spread between quartz plates. ^{1}H NMR (600 MHz) and ^{13}C NMR (150 MHz) spectra were recorded on a Brucker AVANCE-600 at room temperature. Chemical shifts were reported as δ values downfield from an internal standard as tetramethylsilane (Wako Pure Chemical Int. Ltd.) in $CDCl_3$ or sodium 2,2-dimethyl-2-silapentane-5-sulfonate (Merck KGaA) in D_2O. Elemental analysis (carbon, hydrogen, nitrogen) was performed by the Chemical Analysis Centre of the University of Tsukuba.

Synthesis

1,4-Dimethylhomopiperazine (hp′)

This ligand was synthesized by the modified method for the direct methylation of cyclam.[36] A mixed solution of homopiperazine (12.41 g, 0.12 mol), H_2O (15 cm^3), formaldehyde (134 cm^3, 3.50 mol) and formic acid (110 cm^3, 1.58 mol) was refluxed for 24 h at ~175 °C. After cooling, the pH value of the solution was adjusted to 12 by solid NaOH at 25 °C with cooling in an ice bath. Then, the solution was extracted with chloroform (100 cm^3) three times. The organic layer was washed with saturated NaCl aqueous solution (100 cm^3). The resulting solution was dried over anhydrous $MgSO_4$ overnight. After filtering off $MgSO_4$, the solution was concentrated to *ca* 10 cm^3. Distillation of this solution under reduced pressure afforded 1,4-dimethylhomopiperazine. Yield: 80% (12.3 g). ^{1}H NMR ($CDCl_3$): δ 2.67–2.64 (m, 8H, $-CH_2-CH_2-$ and $-CH_2-CH_2-CH_2-$), 2.36 (s, 6H, $-CH_3$), 1.83–1.81 (m, 2H, $-CH_2-CH_2-CH_2-$).

*[$ZnCl_2$(hp′)] (**1**)*

An EtOH (15 cm^3) solution of hp′ (0.52 g, 4.0 mmol) was added slowly to an EtOH solution (20 cm^3) of $ZnCl_2$ (0.55 g, 4.0 mmol). After stirring for 2 h, the solution was filtered. A white powder was obtained (0.29 g, yield: 27%). Colorless crystals suitable for X-ray analysis were obtained by recrystallization from EtOH solution in a refrigerator. IR (cm^{-1}): 2985m, 2961m, 2927m, 2876m, 2821w,

1459s, 1205m, 1117m, 1040vs, 997m, 876w, 743s. Far-IR (cm^{-1}): 485m (ν(Zn–N)), 444w (ν(Zn–N)), 354s, 341m (ν(Zn–Cl)), 313m (ν(Zn–N)), 225w, 205, 181w. Raman (cm^{-1}): 484s (ν(Zn–N)), 444w (ν(Zn–N)), 412m, 388m, 369m, 339m (ν(Zn–Cl)), 310s (ν(Zn–Cl)), 222w, 201w, 188w. (Abbreviations: vs, very strong; s, strong; m, medium; w, weak.) ^{1}H NMR ($CDCl_3$): δ 3.61 (dt, 2H, $-CH_{ax}H-CH_{ax}H-$, $J_{HH} = 5$, 12 Hz), 3.22 (d, 2H, $-CHH_{eq}-CHH_{eq}-$, $J_{HH} = 7$ Hz), 2.73 (d, 2H, $-CH_{ax}H-CH_2-CH_{ax}H-$, $J_{HH} = 7$ Hz), 2.61 (s, 6H, $-CH_3$), 2.50 (m, 2H, $-CHH_{eq}-CH_2-CHH_{eq}-$, $J_{HH} = 6$, 11 Hz), 2.14–2.07 (m, 1H, $-CH_2-CH_{ax}H-CH_2-$), 1.88 (d, 1H, $-CH_2-CHH_{eq}-CH_2-$, $J_{HH} = 16$ Hz). ^{13}C NMR ($CDCl_3$): δ 56.5 (s, $-CH_2-CH_2-$), 51.3 (s, $-CH_2-CH_2-CH_2-$), 46.1 (s, $-CH_3$), 23.4 (s, $-CH_2-CH_2-CH_2-$). Anal. Found: C, 31.59; H, 5.79; N, 10.50. Calc. for $C_7H_{16}Cl_2N_2Zn$: C, 31.79; H, 6.10; N, 10.59%.

*[ZnCl$_3$(Hhp′)] (**1′**)*

The preparation was carried out by the same method as that for **1** using MeOH as a solvent. An MeOH (5 cm^3) solution of hp′ (0.51 g, 4.0 mmol) was added slowly to an MeOH solution (15 cm^3) of $ZnCl_2$ (0.54 g, 4.0 mmol). After stirring for 2 h, the solution was filtered. A white powder was obtained (0.28 g, yield: 23%). Colorless crystals suitable for X-ray analysis were obtained by recrystallization from MeOH solution in a refrigerator. IR (cm^{-1}): 3055vs, 2990m, 2951m, 2883w, 2764w, 1617w, 1467vs, 1391m, 1010s, 783m, 722w. Far-IR (cm^{-1}): 533m (ν(Zn–N)), 490m (ν(Zn–N)), 400m, 359w, 313s (ν(Zn–Cl)), 294s (ν(Zn–Cl)), 281s (ν(Zn–Cl)), 224w. Raman (cm^{-1}): 531m (ν(Zn–N)), 484s (ν(Zn–N)), 438m, 412m, 388m, 369w, 361w, 310s (ν(Zn–Cl)), 292m (ν(Zn–Cl)), 275m (ν(Zn–Cl)), 226w. ^{1}H NMR (D_2O): δ 3.34 (s, 4H, $-CH_2-CH_2-$), 3.21 (t, 4H, $-CH_2-CH_2-CH_2-$, $J_{HH} = 5$ Hz), 2.72 (s, 6H, $-CH_3$), 2.12–2.08 (m, 2H, $-CH_2-CH_2-CH_2-$). ^{13}C NMR (D_2O): δ 58.3 (s, $-CH_2-CH_2-$), 55.0 (s, $-CH_2-CH_2-CH_2-$), 47.1 (s, $-CH_3$), 24.9 (s, $-CH_2-CH_2-CH_2-$). Anal. Found: C, 27.75; H, 5.62; N, 9.24. Calc. for $C_7H_{17}Cl_3N_2Zn$: C, 27.94; H, 5.69; N, 9.31%.

*[ZnBr$_2$(hp′)] (**2**) and [ZnBr$_3$(Hhp′)] (**2′**)*

The preparation of **2** was carried out by the same method as that for **1′** using $ZnBr_2$ (0.90 g, 4.0 mmol) and hp′ (0.53 g, 4.0 mmol). Crystals of **2** (0.18 g, yield: 12%) suitable for X-ray analysis were obtained from hot MeOH solution. On the other hand, colorless crystals of **2′** (0.07 g, yield: 4%) suitable for X-ray analysis were obtained by recrystallization from the resultant MeOH solution in a refrigerator.

2. IR (cm^{-1}): 2988m, 2960m, 2925m, 2874m, 2820w, 1459s, 1203m, 1116m, 1040vs, 996m, 875w, 741s. Far-IR (cm^{-1}): 483s (ν(Zn–N)), 440m (ν(Zn–N)), 390w, 371w, 350s, 265s (ν(Zn–Br)), 243s (ν(Zn–Br)), 208w. Raman (cm^{-1}): 482s (ν(Zn–N)), 448w (ν(Zn–N)), 436w, 410m, 389m, 370m, 349w, 260w (ν(Zn–Br)), 238m (ν(Zn–Br)), 211s. UV–Vis (solid, nm): 204. ^{1}H NMR ($CDCl_3$): δ 3.65 (dt, 2H, $-CH_{ax}H-CH_{ax}H-$, $J_{HH} = 5$, 13 Hz), 3.25 (d, 2H, $-CHH_{eq}-CHH_{eq}-$, $J_{HH} = 7$ Hz), 2.75 (d, 2H, $-CH_{ax}H-CH_2-CH_{ax}H-$, $J_{HH} = 7$ Hz), 2.60 (s, 6H, $-CH_3$), 2.51 (m, 2H, $-CHH_{eq}-CH_2-CHH_{eq}-$), 2.20–2.12 (m, 1H, $-CH_2-CH_{ax}H-CH_2-$), 1.90 (m, 1H, $-CH_2-CHH_{eq}-CH_2-$). ^{13}C NMR ($CDCl_3$): δ 56.6 (s, $-CH_2-CH_2-$), 51.1 (s, $-CH_2-CH_2-CH_2-$), 46.2 (s, $-CH_3$), 23.3 (s, $-CH_2-CH_2-CH_2-$). Anal. Found: C, 23.72; H, 4.64; N, 7.86. Calc. for $C_7H_{16}Br_2N_2Zn$: C, 23.79; H, 4.56; N, 7.93%.

2′. IR (cm^{-1}): 3019vs, 2946m, 2758w, 1631w, 1463vs, 1393m, 1016m, 1005s, 783m, 719w. Far-IR (cm^{-1}): 530m (ν(Zn–N)), 489m (ν(Zn–N)), 440w, 420w, 399s, 335w, 225s (ν(Zn–Br)), 190m (ν(Zn–Br)). Raman (cm^{-1}): 528m (ν(Zn–N)), 490w (ν(Zn–N)), 438w, 418w, 398w, 330w, 218w (ν(Zn–Br)), 189s (ν(Zn–Br)). UV–Vis (solid, nm): 204. ^{1}H NMR (CD_3OD): δ 4.63 (s, 1H, –N*H*), 3.11 (br s, 8H, $-CH_2-CH_2-$ and $-CH_2-CH_2-CH_2-$), 2.64 (s, 6H, $-CH_3$), 2.04 (br s, 2H, $-CH_2-CH_2-CH_2-$). The solubility of **2′** was insufficient to measure its ^{13}C NMR spectrum. Anal. Found: C, 19.46; H, 3.94; N, 6.30. Calc. for $C_7H_{17}Br_3N_2Zn$: C, 19.35; H, 3.95; N, 6.45%.

*[ZnI$_2$(hp′)] (**3**)*

The preparation was carried out by the same method as that for **1′** using ZnI_2 (1.27 g, 4.0 mmol) and hp′ (0.51 g, 4.0 mmol). A white powder was obtained (0.42 g, yield: 23%). Colorless crystals suitable for X-ray analysis were obtained by recrystallization from MeOH solution in a refrigerator. IR (cm^{-1}): 2986m, 2959m, 2923m, 2905m, 2872w, 1460s, 1201m, 1116m, 1038vs, 995m, 874w, 740s. Far-IR (cm^{-1}): 481s (ν(Zn–N)), 439m (ν(Zn–N)), 391w, 370w, 350s, 318w, 243m, 219s (ν(Zn–I)), 198m (ν(Zn–I)). Raman (cm^{-1}): 480s (ν(Zn–N)), 439w (ν(Zn–N)), 410m, 389m, 371m, 347w, 318w, 240m, 217m (ν(Zn–I)), 198s (ν(Zn–I)). UV–Vis (solution, nm (ε, M^{-1} cm^{-1})): 216 (17 300). UV–Vis (solid, nm): 223. ^{1}H NMR ($CDCl_3$): δ 3.72 (dt, 2H, $-CH_{ax}H-CH_{ax}H-$, $J_{HH} = 5$, 13 Hz), 3.29 (d, 2H, $-CHH_{eq}-CHH_{eq}-$, $J_{HH} = 7$ Hz), 2.76 (d, 2H, $-CH_{ax}H-CH_2-CH_{ax}H-$, $J_{HH} = 7$ Hz), 2.57 (s, 6H, $-CH_3$), 2.51 (m, 2H, $-CHH_{eq}-CH_2-CHH_{eq}-$), 2.25–2.18 (m, 1H, $-CH_2-CH_{ax}H-CH_2-$), 1.93 (m, 1H, $-CH_2-CHH_{eq}-CH_2-$). ^{13}C NMR ($CDCl_3$): δ 56.6 (s, $-CH_2CH_2-$), 50.7 (s, $-CH_2-CH_2-CH_2-$), 46.3 (s, $-CH_3$), 23.2 (s, $-CH_2-CH_2-CH_2-$). Anal. Found: C, 18.31; H, 3.76; N, 5.91. Calc. for $C_7H_{16}I_2N_2Zn$: C, 18.79; H, 3.60; N, 6.26%.

*[CdCl$_2$(hp′)]$_n$ (**4**) and [{CdCl$_2$(Hhp′)}$_2$(μ-Cl)$_2$] (**4′**)*

The preparation of **4** was carried out by the same method as that for **1′** using $CdCl_2 \cdot 2.5H_2O$ (0.73 g, 4.0 mmol) and hp′ (0.54 g, 4.0 mmol). Colorless crystals of **4** (0.11 g, yield: 9%) suitable for X-ray analysis were obtained by recrystallization from 2-propanol solution at room temperature. On the other hand, **4′** was obtained as single crystals (0.22 g, yield: 16%) after filtering the white powder **4** and by keeping the filtrate in the refrigerator.

4. IR (cm^{-1}): 2991m, 2960m, 2896m, 2868w, 1456s, 1204m, 1118m, 1043vs, 1008m, 886w, 749m. Far-IR (cm^{-1}): 452s (ν(Cd–N)), 413m (ν(Cd–N)), 380w, 366w, 341m, 232m (ν(Cd–Cl)), 211s (ν(Cd–Cl)), 200s (ν(Cd–Cl)), 169s (ν(Cd–Cl)). Raman (cm^{-1}): 453s (ν(Cd–N)), 420m (ν(Cd–N)), 386m, 363m, 341w, 277w, 246w (ν(Cd–Cl)), 216m (ν(Cd–Cl)), 201w (ν(Cd–Cl)), 168w (ν(Cd–Cl)). ^{1}H

NMR ($CDCl_3$): δ 3.34 (br, 4H, $-CH_2-CH_2-$), 2.58 (s, 8H, $-CH_3$ and $-CH_{ax}H-CH_2-CH_{ax}H-$), 2.48 (br, 2H, $-CH_{eq}H-CH_2-CH_{eq}H-$), 2.24 (br, 1H, $-CH_2-CH_{ax}H-CH_2-$), 2.00 (br, 1H, $-CH_2-CH_{eq}H-CH_2-$). ^{13}C NMR ($CDCl_3$): δ 58.9 (s, $-CH_2-CH_2-$), 54.7 (s, $-CH_2-CH_2-CH_2-$), 48.1 (s, $-CH_3$), 28.0 (s, $-CH_2-CH_2-CH_2-$). Anal. Found: C, 26.70; H, 5.23; N, 8.74. Calc. for $C_7H_{16}CdCl_2N_2$: C, 26.99; H, 5.18; N, 8.99%.

4′. IR (cm^{-1}): 3020vs, 2934w, 2755w, 1632m, 1456vs, 1402m, 1020m, 1005s, 784m, 716w. Far-IR (cm^{-1}): 522m (ν(Cd–N)), 481m (ν(Cd–N)), 439w, 392m, 349w, 311w, 260s (ν(Cd–Cl)), 234s (ν(Cd–Cl)), 194w. Raman (cm^{-1}): 521w (ν(Cd–N)), 477w (ν(Cd–N)), 439m, 424w, 391m, 347w, 327w, 311w, 263m (ν(Cd–Cl)), 234s (ν(Cd–Cl)), 189w. ^1H NMR (CD_3OD): δ 4.73 (s, 2H, $-NH$), 3.10 (br s, 8H, $-CH_2-CH_2-$), 3.04 (t, 8H, $-CH_2-CH_2-CH_2-$, $J_{HH} = 6$ Hz), 2.64 (s, 12H, $-CH_3$), 2.05–2.01 (m, 4H, $-CH_2-CH_2-CH_2-$). ^{13}C NMR (CD_3OD): δ 57.4 (s, $-CH_2-CH_2-$), 55.0 (s, $-CH_2-CH_2-CH_2-$), 46.2 (s, $-CH_3$), 25.7 (s, $-CH_2-CH_2-CH_2-$). Anal. Found: C, 24.25; H, 4.79; N, 7.87. Calc. for $C_{14}H_{34}Cd_2Cl_6N_4$: C, 24.16; H, 4.92; N, 8.05%.

*[{CdBr(hp′)}$_2$(μ-Br)$_2$] (**5**)*

The preparation of **5** was carried out by the same method as that for **1′** using $CdBr_2{\cdot}4H_2O$ (1.38 g, 4.0 mmol) and hp′ (0.52 g, 4.0 mmol). A white powder was obtained (0.93 g, yield: 58%). Colorless crystals suitable for X-ray analysis were obtained by recrystallization from MeOH solution in a refrigerator. IR (cm^{-1}): 2991m, 2960m, 2898m, 2868w, 2819m, 1456vs, 1203m, 1118m, 1042vs, 1008m, 886w, 749m. Far-IR (cm^{-1}): 479m (ν(Cd–N)), 457w, 431w (ν(Cd–N)), 389w, 368w, 271w, 194s (ν(Cd–Br)), 154s (ν(Cd–Br)). Raman (cm^{-1}): 479s (ν(Cd–N)), 453w, 431m (ν(Cd–N)), 389w, 365s, 271w, 192s (ν(Cd–Br)). UV–Vis (solid, nm): 226. ^1H NMR ($CDCl_3$): δ 3.36 (br s, 8H, $-CH_2-CH_2-$), 2.57 (br s, 16H, $-CH_3$ and $CH H_{ax}-CH_2-CH H_{ax}-$), 2.48 (br s, 4H, $-CH H_{eq}-CH_2-CH H_{eq}-$), 2.32 (br s, 2H, $-CH_2-CH_{ax}H-CH_2-$), 2.00 (br, 2H, $-CH_2-CH H_{eq}-CH_2-$). ^{13}C NMR ($CDCl_3$): δ 58.8 (s, $-CH_2-CH_2-$), 54.5 (s, $-CH_2-CH_2-CH_2-$), 48.2 (s, $-CH_3$), 28.2 (s, $-CH_2-CH_2-CH_2-$). Anal. Found: C, 20.71; H, 3.97; N, 6.82. Calc. for $C_{14}H_{32}Br_4Cd_2N_4$: C, 20.99; H, 4.03; N, 6.99%.

*[{CdI(hp′)}$_2$(μ-I)$_2$] (**6**)*

The preparation was carried out by the same method as that for **1′** using CdI_2 (1.36 g, 4.0 mmol) and hp′ (0.52 g, 4.0 mmol). Crystals (0.85 g, yield: 43%) suitable for X-ray analysis were obtained after filtering the white powder and keeping the filtrate in a refrigerator. IR (cm^{-1}): 2988w, 2955m, 2866s, 2819m, 1455vs, 1203w, 1117w, 1040s, 1007m, 885w, 746m. Far-IR (cm^{-1}): 475m (ν(Cd–N)), 431w (ν(Cd–N)), 388w, 366w, 269w, 194w, 161s (ν(Cd–I)), 139w (ν(Cd–I)). Raman (cm^{-1}): 476s (ν(Cd–N)), 431m (ν(Cd–N)), 389w, 364s, 272m, 191m, 161w (ν(Cd–I)). UV–Vis (solution, nm (ε, M^{-1} cm^{-1})): 234 (24 700). UV–Vis (solid, nm): 250. ^1H NMR ($CDCl_3$): δ 3.51 (br s, 4H, $-CH_{ax}H-CH_{ax}H-$), 3.30 (d, 4H, $-CH H_{eq}-CH H_{eq}-$, $J_{HH} = 7$ Hz), 2.64 (d, 4H, $-CH_{ax}H-CH_2-CH_{ax}H-$, $J_{HH} = 7$ Hz), 2.51 (s, 12H, $-CH_3$), 2.48 (br m, 4H, $-CH H_{eq}-CH_2-CH H_{eq}-$), 2.16 (br s, 2H, $-CH_2-CH_{ax}H-CH_2-$), 2.10 (br s, 2H, $-CH_2-CH H_{eq}-CH_2-$). ^{13}C NMR ($CDCl_3$): δ 57.8 (s, $-CH_2-CH_2-$), 52.4 (s, $-CH_2-CH_2-CH_2-$), 47.5 (s, $-CH_3$), 25.9 (s, $-CH_2-CH_2-CH_2-$). Anal. Found: C, 16.77; H, 3.43; N, 5.58. Calc. $C_{14}H_{32}Cd_2I_4N_4$: C, 17.00; H, 3.26; N, 5.66%.

Crystallography

Crystal data and refinement parameters for **1**–**6** are given in Tables 1 and 2. The diffraction data for all complexes except **2** and **5** were measured on a Rigaku/MSC Mercury CCD system with graphite monochromated Mo Kα (λ = 0.710 69 Å) radiation at room temperature for **2′**, **3** and **6**, at −61 °C for **1** and **4′**, at −80 °C for **1′**, and at −92 °C for **4**. All crystals were mounted on glass fiber by epoxy glue. The unit-cell parameters of each crystal were retrieved using Rigaku Daemon software and refined using CrystalClear on all observed reflections.[37] Data using 0.5° intervals in ϕ and ω for 25 s/frame (**1**, **3** and **6**), for 30 s/frame (**1′** and **2′**) and for 60 s/frame (**4** and **4′**) were collected with a maximum resolution of 0.77 Å (744 oscillation images). The highly redundant data sets were reduced using CrystalClear and corrected for Lorentz and polarization effects. An empirical absorption correction was applied for each complex.[37–39] Structures were solved by direct methods using the program SIR 92.[40] The positions of the metal atoms and their first coordination spheres were located from the *E*-map; other non-hydrogen atoms were found in alternating difference Fourier syntheses[41] and least-squares refinement cycles were refined anisotropically during the final cycles (CrystalStructure).[38,39] Hydrogen atoms were placed in calculated positions. The absolute configuration was confirmed from the values of the Flack parameters (0.28(3) for **1** and 0.25(5) for **1′**).[42] Severe disorder was observed around cadmium(II) ion because of insufficient crystal quality of **4**.

For **2** and **5**, the diffraction data were measured on a Rigaku AFC 7S automated four-circle diffractometer with graphite monochromated Mo Kα (λ = 0.710 69 Å) radiation at room temperature. These were mounted on glass fiber by epoxy glue. The unit-cell parameters of each crystal were obtained from a least-squares refinement based on 20 reflections. The intensity of three representative reflections monitored every 150 reflections did not show any decay in either complex. An empirical absorption correction was applied for **2** and **5**.[43] All data were corrected for Lorentz and polarization effects. The structures were solved by direct-methods (SAPI 91)[44] and expanded using Fourier techniques.[45] Non-hydrogen atoms were refined anisotropically. Hydrogen atoms were located on the calculated positions. Refinement was carried out by a full-matrix least-squares method on *F*. All calculations were performed using the teXsan crystallographic software package of the Molecular Structure Corporation.[43]

Crystallographic data have been deposited at the CCDC, 12 Union Road, Cambridge CB2 1EZ, UK, and copies can be obtained on request, free of charge, by quoting the publication citation and the deposition numbers 235 751–235 759.

Table 1. Crystallographic data of zinc complexes (**1**, **1′**, **2**, **2′** and **3**)

Complex	**1**	**1′**	**2**	**2′**	**3**
Detector	CCD	CCD	AFC 7S	CCD	CCD
Formula	$C_7H_{16}Cl_2N_2Zn$	$C_7H_{17}Cl_3N_2Zn$	$C_7H_{16}Br_2N_2Zn$	$C_7H_{17}Br_3N_2Zn$	$C_7H_{16}I_2N_2Zn$
Formula weight	264.50	300.96	353.40	434.32	447.41
Crystal system	Monoclinic	Orthorhombic	Monoclinic	Monoclinic	Monoclinic
Space group	$P2_1$ (no. 4)	$Pna2_1$ (no. 33)	$P2_1/n$ (no. 14)	$P2_1/c$ (no. 14)	$P2_1/n$ (no. 14)
a/Å	7.7392(12)	13.7169(5)	13.904(3)	7.184(6)	7.8375(4)
b/Å	11.146(2)	6.8476(4)	11.828(6)	12.480(10)	12.0992(5)
c/Å	7.2285(12)	13.1673(5)	7.476(3)	14.899(12)	14.3758(8)
β/°	115.655(5)	90	93.92(2)	106.252(9)	94.5908(8)
V/Å^3	562.1(2)	1236.78(10)	1226.6(8)	1282.5(18)	1358.85(12)
Z	2	4	4	4	4
D_{calc}/g cm^{-3}	1.563	1.616	1.914	2.249	2.187
μ(Mo Kα)/cm^{-1}	26.14	25.95	84.95	112.54	63.17
2θ range/°	8–55	8–55	5–55	8–55	8–55
Reflections collected	4075	20 366	3105	10 529	10 061
Unique reflections	1260	1653	2806	2914	2956
R_{int}	0.026	0.022	0.061	0.041	0.030
No. of observations	1226 ($I > 3\sigma(I)$)	1457 ($I > 3\sigma(I)$)	1741 ($I > 2\sigma(I)$)	2046 ($I > 3\sigma(I)$)	1744 ($I > 3\sigma(I)$)
No. of variables	126	135	109	134	125
Final R, R_w[a]	0.029, 0.034	0.020, 0.021	0.052, 0.068	0.049, 0.049	0.040, 0.046
Max/min peak/e$^-$ Å^{-3}	0.28/−0.34	0.29/−0.29	0.61/−1.19	0.95/−0.73	0.74/−0.63

[a] $R = \sum \|F_o| - |F_c\| / \sum |F_o|$; $R_w = [(\sum w(|F_o| - |F_c|)^2 / \sum wF_o^2)]^{1/2}$, $w = 1/\sigma^2(|F_o|)$.

Table 2. Crystallographic data of cadmium complexes (**4**, **4′**, **5** and **6**)

Complex	**4**	**4′**	**5**	**6**
Detector	CCD	CCD	AFC 7S	CCD
Formula	$C_7H_{16}CdCl_2N_2$	$C_{14}H_{34}Cd_2Cl_6N_4$	$C_{14}H_{32}Br_4Cd_2N_4$	$C_{14}H_{32}Cd_2I_4N_4$
Formula weight	311.53	695.99	800.87	988.87
Crystal system	Monoclinic	Monoclinic	Monoclinic	Monoclinic
Space group	$P2_1/c$ (no. 14)	$P2_1/n$ (no. 14)	$P2_1/n$ (no. 14)	$P2_1/n$ (no. 14)
a/Å	6.8864(9)	7.4006(12)	12.507(3)	8.066(11)
b/Å	14.3550(10)	14.030(2)	12.479(3)	12.949(11)
c/Å	11.1831(10)	12.203(2)	7.900(2)	12.98(2)
β/°	90.9710(13)	106.693(6)	95.72(2)	97.986(8)
V/Å^3	1105.3(2)	1213.7(3)	1226.8(5)	1342.8(28)
Z	4	2	2	2
D_{calc}/g cm^{-3}	1.872	1.904	2.168	2.446
μ(Mo$K\alpha$)/cm^{-1}	24.15	24.22	82.75	61.92
2θ range/°	8–55	8–55	5–55	8–55
Reflections collected	6942	8903	3129	10 109
Unique reflections	6792	2558	2819	2869
R_{int}	0.069	0.019	0.026	0.034
No. of observations	4838 ($I > 3\sigma(I)$)	2405 ($I > 3\sigma(I)$)	2239 ($I > 2\sigma(I)$)	2607 ($I > 3\sigma(I)$)
No. of variables	125	135	109	125
Final R, R_w[a]	0.087, 0.089	0.027, 0.035	0.033, 0.043	0.064, 0.108
Max/min peak/e$^-$ Å^{-3}	5.41/−4.38	0.53/−0.48	0.56/−1.10	1.43/−1.00

[a] $R = \sum \|F_o| - |F_c\| / \sum |F_o|$; $R_w = [(\sum w(|F_o| - |F_c|)^2 / \sum wF_o^2)]^{1/2}$, $w = 1/\sigma^2(|F_o|)$.

RESULTS AND DISCUSSION

General aspects

All of the complexes except **1** were prepared by the reaction of an MeOH solution of an equivalent molar hp′ with an MeOH solution of a corresponding metal(II) salt. The initial reaction solution was clear in each case. After several seconds with stirring, the solution became turbid slowly and changed to white. After filtering the white powder, colorless crystals were formed by recrystallization from the filtrate in a refrigerator.

In the case of **1** and **1′**, two coordination types are found in the $ZnCl_2$/hp′ reaction, depending on the solvents used: EtOH for **1** ($ZnCl_2N_2$ type) and MeOH for **1′** ($ZnCl_3N$ type). When $ZnBr_2$ is used as a starting material, the two coordination types **2** ($ZnBr_2N_2$ type) and **2′** ($ZnBr_3N$ type) are obtained by fractional crystallization. In the case of the $CdCl_2$/hp′ reaction, the two coordination types are determined as **4**, a one-dimensional chain structure ($(CdCl_2N_2)_n$ type), and **4′**, which is a dinuclear ($(CdCl_2N)_2(\mu\text{-}Cl)_2$ type). However, the crystal structures of **3**, **5** and **6** are found as only one type, i.e. ZnI_2N_2, $(CdBrN_2)_2(\mu\text{-}Br)_2$ and $(CdIN_2)_2(\mu\text{-}I)_2$ types respectively.

The coordination geometries for all the complexes are classified into five groups, ZnX_2N_2 (**1**, **2**, and **3**), ZnX_3N (**1′** and **2′**), $(CdCl_2N_2)_n$ (**4**), $(CdCl_2N)_2(\mu\text{-}Cl)_2$ (**4′**) and $(CdXN_2)_2(\mu\text{-}X)_2$ (**5** and **6**) as shown in Scheme 2. In summary, the sizes of both the metal and the halide ions influence their structures. Thus, the zinc(II) complexes obtained are only mononuclear and the cadmium(II) complexes are polynuclear or dinuclear, in which two cadmium(II) ions are bridged by two halide ions.

^1H and ^{13}C NMR spectra were measured for all complexes. Each signal of the complexes shifts from that of free hp′ ligand; thus, the coordination of the nitrogen atom of hp′ to the metal(II) ion is expected to be maintained in solution. ^1H NMR spectra of ZnX_2N_2-type complexes (**1**–**3**) are almost the same. Six different protons in the cyclic ring are assigned to three methylene proton pairs with distinction between inside and outside protons. For the $ZnCl_3N$-type complex (**1′**), only three methylene protons are observed and no NH proton is observed in a lower magnetic field because of overlapped D_2O signals. This spectral behavior of **1′** is similar to that of the $(CdCl_2N)_2(\mu\text{-}Cl)_2$ complex (**4′**). On the other hand, the spectral pattern of the $ZnBr_3N$ complex (**2′**) is very different from the spectral patterns of **1**–**3**, **1′** and **4′**. Two broad signals arising from protons on the carbon atoms next to the nitrogen atom (C1, C2, C3 and C5) and from protons on the remaining carbon atom (C4) are observed. For the $(CdCl_2N_2)_n$ (**4**) and $(CdXN_2)_2(\mu\text{-}X)_2$ (**5** and **6**) complexes, ^1H NMR spectra are almost similar to those of ZnX_2N_2 (**1**–**3**). Thus, the difference in coordination geometry is not reflected in their NMR spectra.

Crystal structures

Selected bond distances and angles for all the complexes are given in Tables 3 and 4. All structures reflect the size of the metal(II) ions and halide ions and the difference of each other's polarizability described in terms of HASB (hard and soft acid and base) theory.[1] Representative structures of all the complexes are presented in Fig. 1 (**1** of ZnX_2N_2 type), Fig. 2 (**2′** of ZnX_3N type), Fig. 3 (**4** of $(CdCl_2N_2)_n$ type), Fig. 4

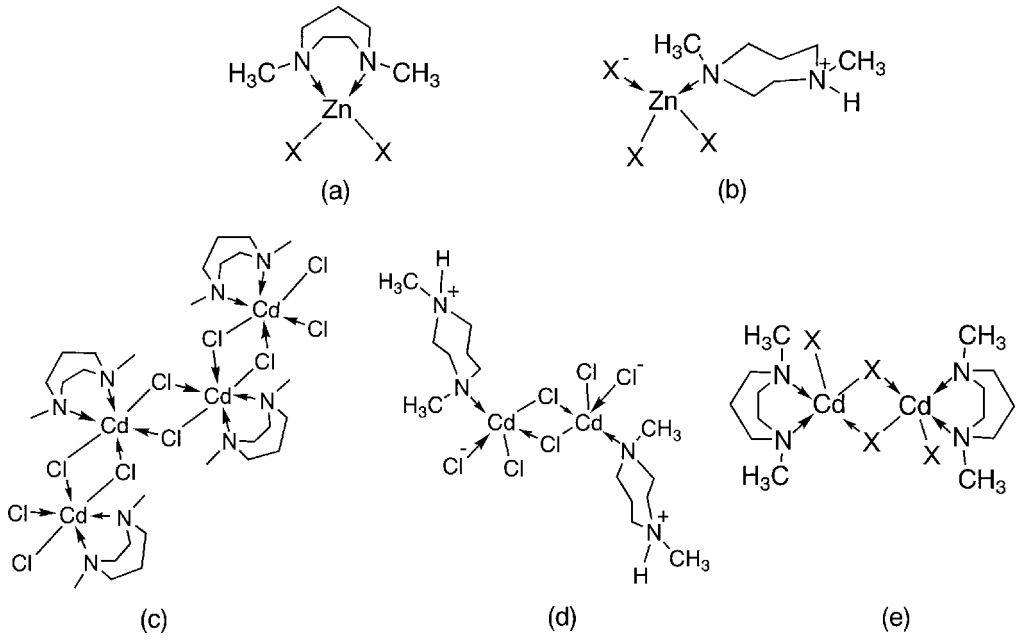

Scheme 2. Five coordination types of complex obtained: (a) ZnX_2N_2 coordination type (X = Cl (**1**), Br (**2**), I (**3**)); (b) ZnX_3N coordination type (X = Cl (**1′**), Br (**2′**)); (c) $(CdCl_2N_2)_n$ one-dimentional chain type (**4**); (d) $CdCl_3N$ coordination type (**4′**); (e) CdX_2N_2 coordination type (X = Br (**5**), I (**6**)).

Table 3. Selected bond distances (Å) and angles (°) for zinc complexes (**1**, **1′**, **2**, **2′** and **3**)

	$[ZnCl_2(hp')]$ (**1**)	$[ZnCl_3(Hhp')]$ (**1′**)	$[ZnBr_2(hp')]$ (**2**)	$[ZnBr_3(Hhp')]$ (**2′**)	$[ZnI_2(hp')]$ (**3**)
Bond distances					
Zn–X1	2.133(2)	2.252(1)	2.331(1)	2.379(1)	2.5243(9)
Zn–X2	2.268(1)	2.2413(9)	2.346(1)	2.412(1)	2.5403(9)
Zn–X3		2.249(1)		2.386(1)	
Zn–N1	2.145(4)	2.105(2)	2.075(7)	2.114(5)	2.068(5)
Zn–N2	2.086(4)		2.079(7)		2.059(6)
Bond angles					
X1–Zn–X2	117.31(6)	113.22(4)	121.27(6)	117.00(4)	120.20(3)
X1–Zn–X3		115.46(3)		110.52(5)	
X2–Zn–X3		109.89(4)		107.90(4)	
X1–Zn–N1	116.2(1)	106.45(8)	117.5(2)	107.7(1)	117.1(2)
X2–Zn–N1	115.01(9)	107.68(6)	107.6(2)	104.5(2)	108.6(1)
X3–Zn–N1		103.32(7)		108.8(1)	
X1–Zn–N2	115.8(1)		114.2(2)		114.5(2)
X2–Zn–N2	110.9(1)		109.3(2)		109.8(2)
N1–Zn–N2	74.2(2)		79.4(3)		79.5(2)

Table 4. Selected bond distances (Å) and angles (°) for cadmium complexes (**4**, **4′**, **5** and **6**)

	$[CdCl_2(hp')]_n$ (**4**)	$[\{CdCl_2(Hhp')\}_2(\mu\text{-}Cl)_2]$ (**4′**)	$[\{CdBr(hp')\}_2(\mu\text{-}Br)_2]$ (**5**)	$[\{CdI(hp')\}_2(\mu\text{-}I)_2]$ (**6**)
Bond distances				
Cd–X1	2.596(3)	2.4508(9)	2.7434(6)	2.870(1)
Cd–X2	2.661(2)	2.4940(7)	2.5460(9)	2.737(1)
Cd–Cl3		2.5123(7)		
Cd–X1′			2.6932(7)	2.973(1)
Cd–Cl1″	2.662(3)			
Cd–Cl2′	2.592(3)			
Cd–Cl3′		2.8123(7)		
Cd–N1	2.415(9)	2.456(2)	2.407(4)	2.44(1)
Cd–N2	2.41(1)		2.382(4)	2.41(1)
Bond angles				
X1–Cd–X2	90.97(9)	113.48(3)	110.54(2)	111.97(4)
Cl1–Cd–Cl3		128.20(3)		
Cl2–Cd–Cl3		117.61(3)		
X1–Cd–X1′			86.36(2)	87.08(3)
Cl1–Cd–Cl1″	83.68(9)			
Cl2–Cd–Cl2′	84.10(8)			
Cl1–Cd–Cl2′	99.3(1)			
X2–Cd–X1′			113.22(3)	112.47(4)
Cl2–Cd–Cl1″	172.5(1)			
Cl1″–Cd–Cl2′	91.62(8)			
Cl3–Cd–Cl3′		79.06(2)		
X1–Cd–N1	162.9(2)	93.43(7)	143.2(1)	91.6(2)
X2–Cd–N1	98.6(2)	92.38(6)	104.4(1)	104.4(3)
X1′–Cd–N1			90.4(1)	140.7(3)
X1′–Cd–N2			140.3(1)	88.2(3)
Cl3–Cd–N1		92.50(6)		
Cl3′–Cd–N1		171.51(6)		
X1–Cd–N2	98.6(2)		89.4(1)	143.2(2)
X2–Cd–N2	90.0(2)		105.2(1)	103.6(2)
N1–Cd–N2	67.4(4)		70.3(1)	70.0(3)

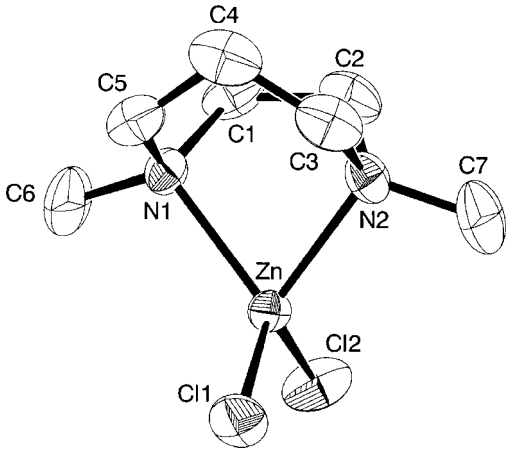

Figure 1. ORTEP diagram of $[ZnCl_2(hp')]$ (**1**). Non-hydrogen atoms are represented with 50% probability ellipsoids.

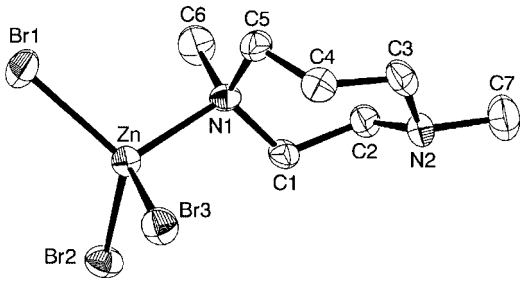

Figure 2. ORTEP diagram of $[ZnBr_3(Hhp')]$ (**2′**). Non-hydrogen atoms are represented with 50% probability ellipsoids.

(**4′** of $(CdCl_2N)_2(\mu\text{-}Cl)_2$ type) and Fig. 5 (**5** of $(CdXN_2)_2(\mu\text{-}X)_2$ type).

On comparing between the series of the ZnX_2N_2 type complexes, the Zn–X distances are seen to increase from **1** (Fig. 1) to **2**, and from **2** to **3** with increasing ionic radii of the halide ions. In addition, the Zn–N distances get shorter from **1** to **2** and those of **2** are also slightly shorter than **3**. However, the bond angles show little change in all the ZnX_2N_2-type complexes. The explanation for this tendency is expected to be as follows. Since the upper limit of the bond angles is assumed to be *ca* 120° for X1–Zn–X2 and *ca* 79° for N1–Zn–N2, both bond angles of **1** are already maxima. Therefore, no characteristic differences in **1**–**3** are observed. ZnX_2N_2-type complexes containing 'simple' didentate N_2 ligands, such as ethylenediamine derivatives, have been reported.[46–53] The crystal structures of **1**, **2** and **3** are the first examples of the ZnX_2N_2 coordination type with a cyclic N_2 ligand.

The structures of **1′** and **2′** (Fig. 2) are of the ZnX_3N type. The bond distances and angles increase with increasing ionic radius. Similar mononuclear structures have been reported for some metals, e.g. manganese(II),[54,55] iron(II),[54] cobalt(II),[24–26,54,56] nickel(II),[54] copper(II),[25,54,56]

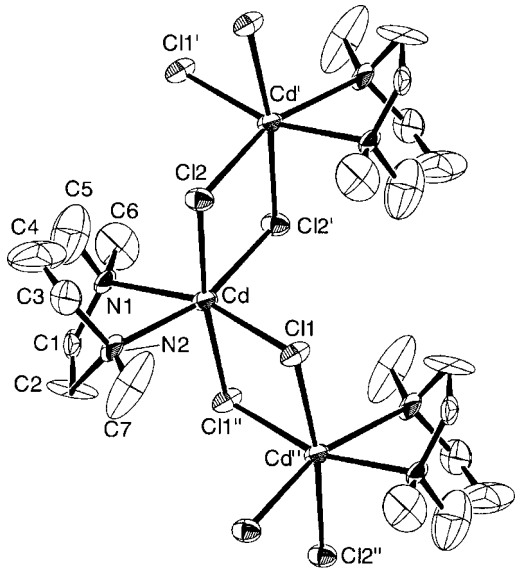

Figure 3. The one-dimensional chain structure of $[CdCl_2(hp')]_n$ (**4**). Non-hydrogen atoms are represented with 50% probability ellipsoids. Severe disorder was observed around the cadmium(II) ion. Symmetry transformations used to generate equivalent atoms: #1 $-x$, $-y$, $-z$; #2 $-x+1$, $-y$, $-z$.

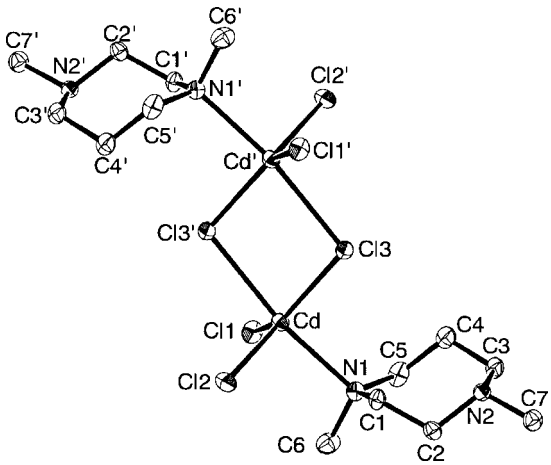

Figure 4. ORTEP diagram of $[\{CdCl_2(Hhp')\}_2(\mu\text{-}Cl)_2]$ (**4′**). Non-hydrogen atoms are represented with 50% probability ellipsoids. Symmetry transformations used to generate equivalent atoms: #1 $-x+2$, $-y+1$, $-z+1$.

zinc(II),[25,28,54,56–59] cadmium(II)[60] and platinum(II)[29] with various ligands, e.g. piperazine, purine, adenine, pyridine and their derivatives.§ Although the zinc(II)[25,28] and cadmium(II)

§ We cannot confirm the source of protons of Hhp′ in **1′**, **2′** and **4′**. Although the analogous protonated ligands have been observed,[25,28,29,54] no reasons were described. One possibility for the proton source is from water included in MeOH. The pH values during the reactions were changed to higher values (pH ~8).

complexes with cyclic N_2 ligands are rare, some analogous complexes have been reported containing piperazine analogues: $[ZnCl_3(HMe_2ppz)]$[25,28] and $[ZnCl_3(H_2Meppz)]$[28] (HMe_2ppz = 1,4-dimethylpiperazinium monocation, H_2Meppz = 1-methylpiperazinium monocation). Both ppz analogue ligands have a six-membered ring, whereas hp′ has a seven-membered ring. The bond distances and angles of $[ZnCl_3(HMe_2ppz)]$[25,28] and $[ZnCl_3(H_2Meppz)]$[28] are almost the same as those of **1′**. Thus, the size of the ring does not relate to their structures. A structural change between **2** and **2′** is observed. It is clear that the MX_3N-type complexes **1′**, **2′** and **4′** (*vide infra*) must have a proton at one nitrogen atom that was not coordinated to central metal(II) ions and exists as Hhp′, since no counter ions are observed by X-ray analysis (see footnote). Moreover, the Zn–Br and Zn–N bond distances of **2** of the $ZnBr_2N_2$ type are shorter than those of **2′** of the $ZnBr_3N$ type. This fact seems to result from the repulsion between the larger bromide ions. In **2**, the Br1–Zn–Br2 angle is extended to 121.27(6)°, whereas the N1–Zn–N2 angle is limited to 79.4(3)° by didentate coordination of hp′. In **2′**, the bond angles around the zinc(II) ion are 104–117°, thus one hp′ ring and three bromide ions are extended equally because of monodentate coordination of Hhp′. On comparison of the ZnX_2N_2 type (**1** and **2**) and ZnX_3N type (**1′** and **2′**), the Zn–X and Zn–N bond lengths in the ZnX_3N type are seen to be longer than those of ZnX_2N_2 type. The bond angles of X–Zn–X and X–Zn–N in the ZnX_3N type are near 109°, which is consistent with an ideal tetrahedral configuration. Thus, the zinc(II) ion in the ZnX_3N coordination mode of **1′** and **2′** takes a nearly ideal tetrahedral configuration and in the ZnX_2N_2 coordination mode of **1** and **2** it takes a distorted tetrahedral configuration.

The crystal structure of **4** reveals that $CdCl_2N_2$ type units are connected by the neighboring chloride ions of another molecule, as shown in Fig. 3. The largest bond angle is Cl1″–Cd–Cl2 (172.5(1)°; symmetry code: $-x+1$, $-y$, $-z$). Thus, the cadmium(II) ion takes a six-coordinated octahedral geometry. The CdX_2N_2-type chain geometry has been reported for the ethylenediamine analogous ligand of *N*,*N*,*N*′,*N*′-tetramethylethylenediamine.[51,61] For the dinuclear structure of **4′**, the central cadmium(II) ions take a nearly trigonal bipyramidal geometry with the $CdCl_4N$ coordination unit containing four chloride ions and one nitrogen atom of hp′, as shown in Fig. 4. The bond angles between chloride ions are from 113° to 128° and those between nitrogen atoms from hp′ and chloride ions are *ca* 90°. In addition, the N1–Cd–Cl3′ angle is 171.51(6)° (symmetry code: $-x+2$, $-y+1$, $-z+1$). The trigonal bipyramidal structure is defined by the fact that the three chloride ions (Cl1, Cl2 and Cl3) form a trigonal plane, and the nitrogen atom from hp′ (N1) and a bridged chloride ion (Cl3′) from another unit exist in the axial position. Two hp′ ligands exist in alternate directions. Two cadmium(II) ions and two bridged chloride ions form a plane. Every $Cd-Cl_{ter}$ distance is almost the same and the $Cd-Cl_{brid}$ distance is longer than that of the $Cd-Cl_{ter}$ distance. The only example of CdX_3N type has been reported for $[CdBr_3(HL)]$ (HL = *N*-benzylpiperazinium monocation), containing three bromide ions and one piperazine derivative.[60] This complex is a mononuclear complex, but two units have some interactions by an intermolecular hydrogen bonding between one bromide ion and the proton of the cationic nitrogen atom.

The dinuclear complexes **5** (Fig. 5) (symmetry code: $1-x$, $1-y$, $1-z$) and **6** (symmetry code: $-x$, $-y$, $-z$) have the CdX_3N_2 type structure (X = Br (**5**) and I (**6**)). In **5** and **6**, two halide ions bridge two cadmium(II) ions, thus the cadmium(II) ions take a five coordination by two nitrogen atoms from hp′ and three halide ions. The chloride ion is supposed to be too small to form a dinuclear complex as $(CdClN_2)_2(\mu\text{-}Cl)_2$. The two bridged halide ions and two cadmium(II) ions form a plane that is almost square. When the dinuclear complex is thought of as separated into mononuclear parts, each CdX_2N_2 type has a large distortion, as indicated by the bond angles, e.g. *ca* 143° for X1–Cd–N1, *ca* 90° for X1–Cd–N2 and 104° for X2–Cd–N1 and X2–Cd–N2. The vacant position is occupied by the bridged halide ion from another unit. The differences in the bond angles between **5** and **6** show the same tendency as those of the ZnX_2N_2-type complexes (**1**, **2** and **3**). The average Cd–X distances of **6** are longer than those of **5** and increase with increasing ionic radii of the halide ions. Some structural analogous dinuclear complexes containing five-coordinated cadmium(II) ions have been reported.[62–64] In these reported complexes, the chelating ligands contain an aromatic or imidazole ring, and the central cadmium(II) ions take a distorted trigonal bipyramidal geometry. In the case of **5** and **6**, each cadmium(II) ion also takes a distorted trigonal bipyramidal geometry.

As shown in Scheme 2, when the size of the metal(II) or halide ion is small, e.g. zinc(II) or chloride ion, then the MX_3N type is preferred. The MX_2N_2 coordination type is preferred to the MX_3N type with increasing ion sizes, e.g. cadmium(II) and iodide ions. In the case of the pairs zinc(II)/Cl^- (**1** and **1′**), zinc(II)/Br^- (**2** and **2′**) and cadmium(II)/Cl^- (**4**

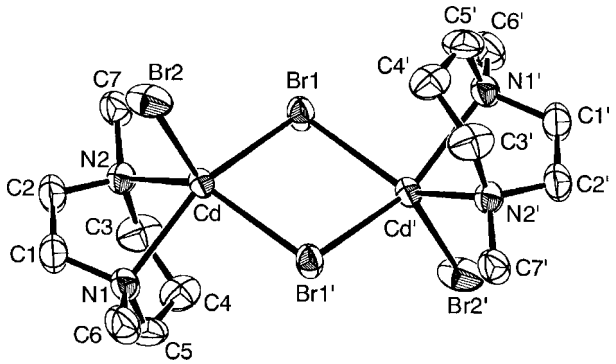

Figure 5. ORTEP diagram of $[\{CdBr(hp')\}_2(\mu\text{-}Br)_2]$ (**5**). Non-hydrogen atoms are represented with 50% probability ellipsoids. Symmetry transformations used to generate equivalent atoms: #1 $1-x$, $1-y$, $1-z$.

and **4′**), they can occur as both the MX_3N and MX_2N_2 types. We suppose that all complexes prefer the MX_3N coordination type to the MX_2N_2 coordination type. This is because the tight didentate coordination of hp′ to the metal ion (MX_2N_2) is very unstable (kinetically stable) and the complexes formed tend to the configuration with less distortion (MX_3N) (thermodynamically stable). On the other hand, bromide and iodide ions cannot take up the MX_3N type because of the repulsions between the larger halide ions. The formation of dinuclear cadmium(II) complexes can be expected to occur in two steps as follows. First, the mononuclear complex of CdX_2N_2 type forms as described above. However, the cadmium(II) ion is too large to exist as a mononuclear complex with hp′ and larger halide ions; therefore, they take up five coordination. Second, these are stable as polynuclear or dinuclear complexes through coordination of the sixth ligand in the vacant position. The larger ionic radius of the cadmium(II) ion compared with that of zinc(II) ion contributes more to the structure being obtained as mononuclear or dinuclear.

Spectroscopic studies

IR spectra in the 4600–400 cm^{-1} region were measured for all complexes. In the 3000–2800 cm^{-1} region, some bands arising from the aliphatic alkyl group are observed. The spectral pattern in that region reflects the MX_3N and the MX_2N_2 types. In the spectra of the MX_3N type, one strong band and some weak bands are observed in the 3060–2750 cm^{-1} region, whereas some bands with a medium strength are observed in the spectra of the MX_2N_2 type. In addition, a large number of bands are observed in the 1630–900 cm^{-1} region arising from the hp′ ligand.

The measurements of far-IR spectra and FT-Raman in the 650–150 cm^{-1} region were performed for all complexes, and some metal–ligand stretching bands were found. The far-IR spectra of ZnX_2N_2 type (**1, 2** and **3**) and MX_3N type (**1′**, **2′** and **4′**) are shown in Figs 6 and 7 respectively. When the spectra of **1** and **2** are compared, the ν(Zn–N) bands are expected theoretically to show small shifts and the ν(Zn–X) bands are expected to show large shifts to lower energy in going from the chloro complex **1** to the bromo complex **2** because only **1** and **2** have different halide ions.[65] In this context, the bands, that show large shifts from **1** to **2**, and from **2** to **3**, are assigned to ν(Zn–X): 341, 313 cm^{-1} for **1**, 265, 243 cm^{-1} for **2**, and 219, 198 cm^{-1} for **3**.

For the MX_3N coordination type, the strong absorption bands, which show large shifts from **1′** (313–281 cm^{-1}) to **2′** (*ca* 225 cm^{-1}), are assigned to ν(Zn–Cl) and ν(Zn–Br) respectively. Although **4′** has a dinuclear structure, the spectra of **1′** and **4′** in the 600–390 cm^{-1} region are very similar, and the strong bands at 260 and 234 cm^{-1} in the spectrum of **4′** are thought to be shifted from the bands at 313–281 cm^{-1}, just like in that of **1′**. Complex **4′** contained two types of halide ion, i.e. bridging and terminal. Thus, two or more complicated bands are supported to show correspond to $\nu(Cd-Cl)_{ter}$ and

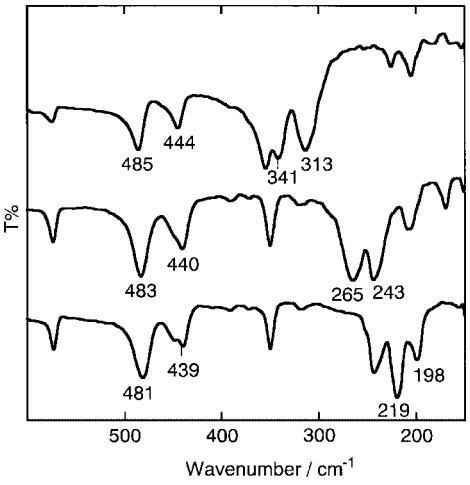

Figure 6. Far-IR spectra of the complexes which have the ZnX_2N_2 coordination type (upper: **1**; middle: **2**; lower: **3**).

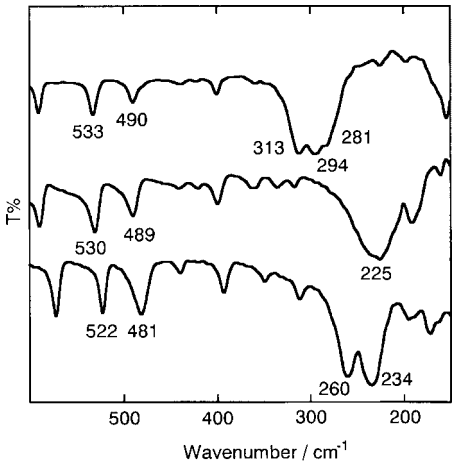

Figure 7. Far-IR spectra of the complexes which have the MX_3N coordination type (upper: **1′**; middle: **2′**; lower: **4′**).

$\nu(Cd-Cl)_{brid}$. The energy of $\nu(Cd-Cl)_{ter}$ should be lower than that of $\nu(Cd-Cl)_{brid}$.[46] In general, ν(Cd–Cl) is observed near 250 cm^{-1} in the literature.[12,13] Thus, the bands at 260 and 234 cm^{-1} are assigned to ν(Cd–Cl) in the spectra of **4′** without distinction from $\nu(Cd-Cl)_{ter}$ and $\nu(Cd-Cl)_{brid}$. For **5** and **6**, the bands of ν(Cd–X) (X = Br and I) are also assigned in the same way. The spectra of **5** and **6**, having the $(CdXN_2)_2(\mu\text{-}X)_2$ type structure, are different from the spectrum of **4**, although the $(CdXN_2)_2$ unit bridging X is included in **4, 5** and **6**. Raman spectral patterns of all the complexes except **4** are very similar to the far-IR spectral patterns. Thus, these spectra support that the crystal structure of **4** has a one-dimensional chain structure and the central cadmium(II) ion takes an octahedral geometry as shown in crystal structure. In the far-IR spectrum of **4**, a complicated set of four peaks was observed because of this structure.

The ν(M–N) bands for all complexes are assigned in the 550–430 cm^{-1} region. Two strong bands are observed in this region, and these are almost at the same positions in the same series. The assignments of the ν(M–N) bands have been studied by using 'simple' complexes containing only ammonia, pyridine, and imidazole, and by large-molecular-weight complexes containing multidentate ligands. The values of the ν(M–N) bands in the literature are separated into two types, i.e. 430–370 cm^{-1} for ammine complexes $[ZnX_2(NH_3)_2]$[14] (X = Cl, Br and I) and $[M(NH_3)_4]$[65] (M = Zn and Cd), and 280–220 cm^{-1} for imidazole and pyridine complexes $[ZnX_2L_2]$ (L = imidazole[14] and pyridine[15]) and piperazine complexes $[ZnCl_3(H_2Meppz)]$ and $[ZnCl_3(HMe_2ppz)]$.[28] However, in our results there are no significant bands in the 280–220 cm^{-1} region, as shown in Figs 6 and 7. Therefore, the ν(M–N) in the spectra of all complexes are assigned in the 550–430 cm^{-1} region. Accordingly, the ν(M–N) and ν(M–X) stretching bands influence each coordination structure.

The absorption spectra of **1**–**6** were measured in both solution (MeOH and MeCN) and the solid state. In both MeOH and MeCN solutions, only iodo complexes **3** and **6** show a broad peak. The peak maximum of **3** has almost the same energy in both solvents (216 nm in MeCN and 220 nm in MeOH). In the case of **6**, only one band at 240 nm is observed in both solvents. An additional study was carried out in the solid state. The bromo complexes **2**, **2′** and **5** show one band below 230 nm in the solid state. We expect that the differences of each coordination mode between **2** and **2′** reflect their absorption spectra. However, both spectra show the band at the same energy; thus, we cannot find any differences. The chloro complexes **1**, **1′**, **4** and **4′** also have no bands, even in the solid state. The observed bands are shifted from iodo complexes to bromo and chloro complexes in each metal(II) series. Thus, these bands are expected to relate to the CT transition bands between the halide ions and each metal(II) ion. In addition, the CT transition bands between the nitrogen atom and the metal(II) ions do not appear above 200 nm. The discussion about ligand-to-metal CT (LMCT) transition bands gives new insights into the study of zinc(II) and cadmium(II) complexes. There are no assignments of LMCT transition bands in the reported zinc(II) and cadmium(II) complexes exactly because the ligands containing aromatic rings or multiple bonds interfere with the LMCT transition bands.

CONCLUSIONS

Zinc(II) and cadmium(II) complexes with the 'simple' supporting ligand hp′ have been synthesized to obtain more insight into the model complexes and the physicochemical characterizations, such as stretching vibration energy and LMCT transition band energy. The complexes obtained show five coordination types: ZnX_2N_2 (**1**, **2** and **3**), ZnX_3N (**1′** and **2′**), $(CdCl_2N_2)_n$ (**4**), $(CdCl_2N)_2(\mu\text{-}Cl)_2$ (**4′**) and $(CdXN_2)_2(\mu\text{-}X)_2$ (**5** and **6**). The differences in both ionic radius (metal ions and halide ions) and polarizability contribute a great deal to their structural types. These results suggest a number of things about the synthetic model complexes. One is that a bidentate ligand with a coordinated nitrogen atom is useful for stabilizing the zinc(II) and cadmium(II) complexes without an aromatic ring or a multiple bond. Another is that suitable combinations of metals and halide ions can be used to design the complex. For example, in order to keep a bidentate mode and a monodentate complex, we have to choose zinc(II) as a central metal ($ZnCl_2$/hp′, $ZnBr_2$/hp′ and ZnI_2/hp′). In addition, it becomes clear that the cadmium(II) ion prefers to form a dinuclear or polynuclear complex bridged by halide ions.

Typical ν(M–N) and ν(M–X) peaks for the five structural types are clearly observed around 540–410 cm^{-1} and 350–160 cm^{-1} respectively. Therefore, the different structures can be distinguished clearly by far-IR and Raman spectra. In the UV–Vis absorption spectra, the LMCT transition bands between halide ions and metal(II) ions are observed for bromo and iodo complexes in the 204–250 nm region. The LMCT transition bands related to the coordination nitrogen atoms are expected to exist below 200 nm. We obtained the same results from zinc(II) and cadmium(II) analogous complexes with (−)-spartein (sp) as a bidentate ligand (Matsunaga *et al*, unpublished data), and the crystal structure of $[ZnBr_2(sp)]$ has been reported by Lee *et al*.[66] These complexes also have the same MX_2N_2-type (M = Zn(II), Cd(II); X = Cl, Br, I) structure as **1**, **2** and **3**. These results suggest that the complexes with didentate ligands give LMCT transition bands exactly in the near-UV region. In this context, further studies to design and synthesize MS_2N_2, MS_2O_2 and MO_2N_2 (M = Zn(II), Cd(II)) coordination-type complexes that just contain 'simple' ligands are currently in progress. Therefore, this methodology is useful for collecting information about zinc(II) and cadmium(II) complexes directly.

In this study, we found that two pairs of metal(II) ions and halides (zinc(II)/B_r^- and cadmium(II)/Cl^-) show structural changes during recrystallization. These fundamental studies are also useful for determining metal–ligand coordination environments in biological systems and coordination chemistry.

Acknowledgements

We thank Professor K. Tanaka of the Institute of Molecular Science for FT-Raman measurements. This research was in part supported by Grant-in-Aid for Scientific Research (nos 13555257 and 14540510) from the Japan Society for the Promotion of Science and the 21st Century COE program from the Ministry of Education, Culture, Sports, Science and Technology.

REFERENCES

1. Shriber DF, Atkins PW. *Inorganic Chemistry*, 3rd edn. Oxford University Press: New York, 1999.
2. Cotton FA, Wilkinson G, Murillo CA, Bochmann M. *Advanced Inorganic Chemistry*, 6th edn. John Wiley: New York, 1999.

3. Cowan JA. *Inorganic Biochemistry*, 2nd edn. Wiley–VCH: New York, 1996.
4. Lippard SJ, Berg JM. *Principles of Bioinorganic Chemistry*. University Science Books: Mill Valley, 1994.
5. Huheey JE, Keiter EA, Keiter RL. *Inorganic Chemistry*, 4th edn. HarperCollins College Publishers: New York, 1993.
6. Moszczenski CW, Hooper RJ. *Inorg. Chim. Acta* 1983; **70**: 71.
7. Sabatini A, Sacconi L. *J. Am. Chem. Soc.* 1964; **86**: 17.
8. Frigerio A, Halac B, Perec M. *Inorg. Chim. Acta* 1989; **164**: 149.
9. Aitken GB, Duncan JL, McQuillan GP. *J. Chem. Soc. Dalton Trans.* 1972; 2103.
10. Day P, Seal RH. *J. Chem. Soc. Dalton Trans.* 1972; 2054.
11. Vasak M, Kagi JHR, Hill HAO. *Biochemistry* 1981; **20**: 2852.
12. Adams DM, Chatt J, Davidson JM, Gerratt J. *J. Chem. Soc. Dalton Trans.* 1963; 2189.
13. Goggin PL, Goodfellow RJ, Kessler K. *J. Chem. Soc. Dalton Trans.* 1977; 1914.
14. Perchard C, Novak A. *Spectrochim. Acta* 1970; **26A**: 871.
15. Saito Y, Cordes M, Nakamoto K. *Spectrochim. Acta* 1972; **28A**: 1459.
16. Henkel G, Krebs B. *Chem. Rev.* 2004; **104**: 801.
17. Salas JM, Romero MA, Rahmani A, Faure R, Alvarez de Cienfuegos G, Tekink ERT. *J. Inorg. Biochem.* 1996; **64**: 259.
18. Baggio R, Garland MT, Perec M. *J. Chem. Soc. Dalton Trans.* 1993; 3367.
19. Burth R, Vahrenkamp H. *Inorg. Chim. Acta* 1998; **282**: 193.
20. Wilker JJ, Lippard SJ. *J. Am. Chem. Soc.* 1995; **117**: 8682.
21. Corwin Jr DT, Koch SA. *Inorg. Chem.* 1988; **27**: 493.
22. Sun WY, Zhang L, Yu KB. *J. Chem. Soc. Dalton Trans.* 1999; 795.
23. Matsunaga Y, Fujisawa K, Ibi N, Amir N, Miyashita Y, Okamoto K. Submitted to *Bull. Chem. Soc. Jpn*.
24. Clemente DA, Marzotto A, Valle G, Visona CJ. *Polyhedron* 1999; **18**: 2749.
25. Perry WD, Quagliano JV, Vallarino LM. *Inorg. Chim. Acta* 1973; **7**: 175.
26. Marcotrigiano G. *Inorg. Chim. Acta* 1978; **26**: 57.
27. Marcotrigiano G, Menabue L, Pellacani GC. *Inorg. Chem.* 1976; **15**: 2333.
28. Clemente DA, Marzotto A, Benetollo F. *Polyhedron* 2002; **21**: 2161.
29. Ciccarese A, Clemente DA, Fanizzi FP, Marzotto A, Valle G. *Inorg. Chim. Acta* 1998; **275–276**: 410.
30. Ciccarese A, Clemente DA, Fanizzi FP, Marzotto A, Valle G. *Inorg. Chim. Acta* 1998; **275–276**: 419.
31. Hagiwara M, Narumi Y, Kindo K, Nishida T, Kaburagi M, Tonegawa T. *Physica B* 1998; **246–247**: 234.
32. Chiari B, Piovesana O, Tarantelli T, Zanazzi PF. *Inorg. Chem.* 1990; **29**: 1172.
33. Ali MS, Whitmire KH, Toyomasu T, Siddik ZH, Khokhar AR. *J. Inorg. Biochem.* 1999; **77**: 231.
34. Allen GW, Ling ECH, Krippner LV, Hambley TW. *Aust. J. Chem.* 1996; **49**: 1301.
35. Fukaya A, Higemoto W, Hagiwara M, Nagamine K. *Physica B* 2000; **289–290**: 189.
36. Barefield EK, Wagner F. *Inorg. Chem.* 1973; **12**: 2435.
37. Pflugrath JW. *Acta Crystallogr. Sect. D* 1999; **55**: 1718.
38. CrystalStructure 3.51: Crystal Structure Analysis Package: Rigaku and Rigaku/MSC, 2003.
39. Watkin DJ, Prout CK, Carruthers JR, Betteridge PW. Crystal Issue 10, Chemical Crystallography Laboratory, Oxford, UK, 1996.
40. Altomare A, Cascarano G, Giacovazzo C, Guagliardi A, Burla M, Polidori G, Camalli M. *J. Appl. Crystallogr.* 1994; **27**: 435.
41. Beurskens PT, Admiraal G, Beurskens G, Bosman WP, de Gelder R, Israel R, Smits JMM. The DIRDIF-99 program system. Technical report of the Crystallography Laboratory, University of Nijmegen, The Netherlands, 1999.
42. Flack HD. *Acta Crystallogr. Sect. A* 1983; **39**: 876.
43. teXsan: Single Crystal Structure Analysis Package, Version 1.10b Molecular Structure Corporation, The Woodlands, TX, 1999.
44. Fan HF. SAPI 91: Structure Analysis Programs with Intelligent Control. Rigaku Corporation, Tokyo, Japan, 1991.
45. Beurskens PT, Admiraal G, Beurskens G, Bosman WP, de Gelder R, Israel R, Smits JMM. The DIRDIF-94 Program System. Technical report of the Crystallography Laboratory, University of Nijmegen, The Netherlands, 1994.
46. Cariati F, Ciani G, Menabue L, Pellacani GC, Rassu G, Sironi A. *Inorg. Chem.* 1983; **22**: 1897.
47. Htoon S, Ladd MFC. *J. Cryst. Mol. Struct.* 1973; **3**: 95.
48. Htoon S, Ladd MFC. *J. Cryst. Mol. Struct.* 1974; **4**: 357.
49. Amirnasr M, Mahmoudkhani AH, Gorji A, Dehghanpour S, Bijanzadeh HR. *Polyhedron* 2002; **21**: 2733.
50. Bennett AMA, Foulds GA, Thornton DA, Watkins GM. *Spectrochim. Acta A* 1990; **46A**: 13.
51. Abraham MH, Parrett FW. *Can. J. Chem.* 1970; **48**: 181.
52. Amirnasr M, Schenk KJ, Salavati M, Dehghanpour S, Taeb A, Tadjarodi A. *J. Coord. Chem.* 2003; **56**: 231.
53. Mitra S, Kundu P, Singh RB. *Thermochim. Acta* 1994; **236**: 175.
54. Quagliano JV, Banerjee AK, Goedken VL, Vallarino LM. *J. Am. Chem. Soc.* 1970; **92**: 482.
55. Birdy RB, Brun G, Goodgame DML, Goodgame M. *J. Chem. Soc. Dalton Trans.* 1979; 149.
56. Darby WL, Vallarino LM. *Inorg. Chim. Acta* 1983; **75**: 65.
57. Purnell LG, Hodgson DJ. *J. Am. Chem. Soc.* 1977; **99**: 3651.
58. Sheldrick WS. *Z. Naturforsch, Treil B* 1982; **37**: 653.
59. Bencini A, Borghi E. *Inorg. Chim. Acta* 1987; **135**: 85.
60. Bruni S, Cariati F, Pozzi A, Battaglia LP, Corradi AB. *Inorg. Chim. Acta* 1991; **183**: 221.
61. Htoon S, Ladd MFC. *J. Cryst. Mol. Struct.* 1974; **4**: 97.
62. Long GV, Boyd SE, Harding MM, Buys IE, Hambley TW. *J. Chem. Soc. Dalton Trans.* 1993; 3175.
63. Matthews CJ, Clegg W, Heath SL, Martin NC, Hill MNS, Lockhart JC. *Inorg. Chem.* 1998; **37**: 199.
64. Mague JT, Krinsky JL. *Inorg. Chem.* 2001; **40**: 1962.
65. Nakamoto K. *Infrared and Raman Spectra of Inorganic and Coordination Compounds Part B*. Wiley Interscience: New York, 1997.
66. Lee YM, Kang SK, Kim YI, Choi SN. *Acta Crystallogr. Sect. C* 2002; **58**: m453.

